Available online at www.sciencedirect.com
ScienceDirect
European Polymer Journal 43 (2007) 4602–4612
EUROPEAN POLYMER JOURNAL
www.elsevier.com/locate/europolj

Macromolecular Nanotechnology

Sequential polymer lithography for chemical sensor arrays

Maria Kitsara [a,b], Konstantinos Beltsios [b], Dimitrios Goustouridis [a], Stavros Chatzandroulis [a], Ioannis Raptis [a,*]

[a] *Institute of Microelectronics, NCSR "Demokritos", 15310 Athens, Greece*
[b] *Materials Science and Engineering Department, University of Ioannina, Ioannina 45110, Greece*

Received 4 April 2007; received in revised form 3 June 2007; accepted 25 July 2007
Available online 3 August 2007

Abstract

A simple process for the deposition of up to six different polymers in selected areas to be used as sensitive layers in chemical sensor arrays is presented. The process is based on photolithographic processes and takes advantage of the balance between UV exposure dose, material tone and developers used. The sensing properties of the deposited films in the array were characterized by the in situ monitoring of volume expansion upon exposure to analytes using white light reflectance sspectroscopy. The swelling properties of processed films are compared to the unprocessed ones for the purpose of examining the variation induced by the processing steps (exposure and development circles). Additionally, the repeatability of the processes as well as the effect of analyte sequence is examined. This process offers good control of the lateral dimensions and the thickness of the polymeric films and allows for the parallel fabrication of sensors based on different transduction mechanisms including mass sensitive and stress induced bending chemical sensors.

Keywords: Polymer deposition; Photolithography; Chemical sensors; Vapor sorption; Polymer swelling

1. Introduction

One of the most important problems in chemical sensor fabrication is the deposition of the chemically sensitive materials on the transducer [1]. This problem becomes even more serious in the case of deposition of different sensitive materials in the form of sensor arrays. Arrays of chemical sensors with partially overlapping selectivity can be utilized as an electronic signature to characterize a wide range of odors and other volatile compounds by pattern-recognition means [2].

For example, in the fabrication of conductive polymer array sensors, thin polymer films of either specialized conductive polymers [3] or composites based on ordinary polymers and conductive fillers need to be deposited in stripe form on the same substrate. In these sensors, the resistance of each polymer stripe changes in accordance to the volatile compound concentration in their ambient [4,5]. Other chemically sensitive devices requiring the selective deposition of polymer films include capacitive type chemical sensors where polymer films have

* Corresponding author. Tel.: +30 210 650 3265; fax: +30 210 651 1723.
E-mail address: raptis@imel.demokritos.gr (I. Raptis).

0014-3057/$ - see front matter © 2007 Elsevier Ltd. All rights reserved.
doi:10.1016/j.eurpolymj.2007.07.034

to be selectively placed between electrodes in order to form an array of capacitors whose capacitance changes in accordance to analyte concentration [6]. Another example is offered by silicon/polymer bimorph chemical sensing arrays operating either in resonance or static bending. These devices require the selective deposition and patterning of different sensitive polymer films on to a flexible member part of silicon [7] or silicon nitride [8]. In these devices the stress induced on the flexible member as the overlying polymer swells in the presence of analyte molecules results in the change of resonance frequency [9] and/or bending [10,11].

Polymeric materials are usually applied to sensor devices through solution-based methods such as spin coating, spray coating, dip coating, drop casting and ink-jet printing [12,13]. Electrochemical deposition is a technique used mainly for the formation of conducting polymer films [14]. Langmuir–Blodgett (LB) film deposition method leads to sensing layers made of lipids, polymers or lipid-polymer blends [15], while a related method is that of the deposition of self-assembled monolayers (SAMs) [16]. Vacuum deposition techniques are also possible methods of obtaining thin polymer films including mostly sputtering [17], plasma polymerization [18], physical vapor deposition [19], and a recent technique named matrix-assisted pulsed laser evaporation [20]. Among the aforementioned methods: (a) those making use of solutions based methods lack in pattern precision and repeatability, and the problems become more severe as the demand for smaller, more complex sensors increases, (b) those from electrochemical deposition to the end are severely limited as regards the selection of deposited materials.

In the present work a new approach allowing for the application of more than one sensitive polymer layers using conventional lithographic techniques only is proposed. Photolithography has already proved its usefulness in the fabrication of chemical sensors where carbosiloxane polymeric layers are patterned on defined areas of surfaces using photoactivated catalyst and hydrosilylation chemistry [21]. Here the deposition of six photosensitive polymeric materials on the same substrate by applying exclusively photolithographic techniques is demonstrated. The process is a delicate balance between exposure dose for each exposure step, material tone (negative/positive) and developers used. The use of lithographic processes allows for the definition of polymeric films at the desired layout and for a wide film thickness range. Also, it is a parallel, at the wafer level, process, compatible with microelectronic processes and, as a result, a low-cost one.

A variety of polymers have been examined as candidates for deposition and the selection of the six final deposited was based on criteria to be described in the Section 3.1. The response of the deposited polymer array is characterized through swelling measurements for each polymer film in the presence of selected analytes (methanol, ethanol, toluene vapors and humidity) by White Light Reflectance Spectroscopy (WLRS), also described as multi wavelength interferometry [22]. The effect of each layer deposition on the swelling properties of the previous layers is also studied, as it is preferable that the properties of already deposited polymer films do not change appreciably after the addition of each new layer.

2. Experimental

2.1. Materials

For the fabrication of the polymeric array, six photosensitive materials are deposited. All selected materials are sensitive to irradiation in the DUV spectrum and are either homopolymers or photoresists (commercial and experimental ones). The photosensitive materials to be used are prepared in appropriate solutions as following:

(a) *EPR*: Consisting of epoxy polymer from Shell [23] (8% w/w in ethyl-(*S*)-lactate, from Sigma–Aldrich) and 1% w/w UVI6974 (Union Carbide) photoacid generator.
(b) *PDMS*: Siloxane from UCT (PS264) [24] and chemical composition 94.5% PDMS, copolymer 5% diphenyl siloxane, copolymer 0.5% methyl-vinyl-siloxane and $M_w = 990$ K (3% w/w in methyl iso butyl ketone, MIBK from Merck).
(c) *PMMA* with $M_w = 120$ K [25] from Du Pont, (5% w/w in propylene glycol methyl ether acetate, PGMEA, from Sigma–Aldrich).
(d) *PHEMA* negative: It is based on PHEMA polymer $M_w = 300$ K [26], from Sigma–Aldrich (4% w/w in ethyl-(*S*)-lactate) and 2% TPS-SbF_6 (General Electric) photoacid generator.
(e) *SAL-601* [27] from Shipley (diluted in MIBK in a 1:2 ratio),
(f) *UVIII* [28] from Shipley (diluted in ethyl-(*S*)-lactate in a 1:1 ratio).

The chemical types of the main polymers of the photosensitive materials are illustrated in Fig. 1. Using the above solutions and appropriate spin coating conditions the film thicknesses obtained fall in the 110–150 nm range; it has been demonstrated that the fractional swelling is independent for this film thickness range [29]. For the DUV exposures, a broadband Hg–Xe lamp (Oriel) was used. In the case of PHEMA negative, a filter at 248.9 nm was used.

2.2. Measurement set-up

For the measurement of the polymeric film thickness changes due to absorption and desorption of analytes an experimental set-up (Fig. 2) combining a WLRS setup, a delivering subsystem for controlled concentrations of analyte and the measuring chamber was used. In the analyte-delivering unit initially dry nitrogen flux is split in a carrier and a diluting part with the help of two mass flow controllers. The carrier is bubbled through the volatile compound of interest and subsequently mixed with the diluting part to achieve the desired concentration level in the measuring chamber. The current set-up offers four bubblers and four valves and the user can select the analyte of interest. The chamber volume is ~150 ml and the gas flow is 1000 ml/min; thus saturation within the chamber is reached quickly. The temperature in the gas delivering subsystem and in the measuring chamber is kept constant at 30 ± 0.5 °C.

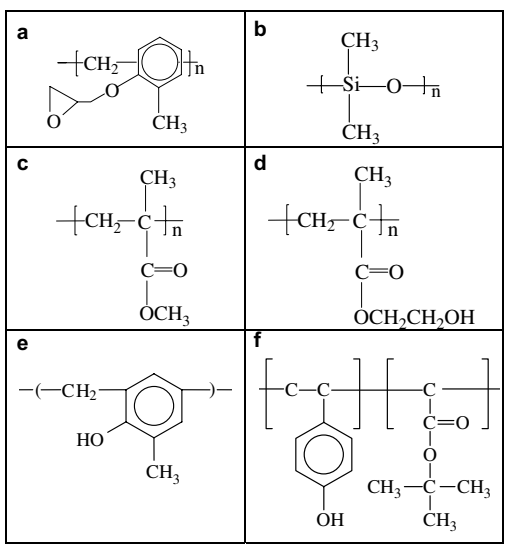

Fig. 1. Chemical types of the polymeric materials of the array: (a) epoxydised novolac of EPR, (b) PDMS, (c) PMMA, (d) PHEMA, (e) novolac of SAL-601, and (f) UVIII.

In the WLRS subsystem, a splitter optical fiber is connected to a VIS-NIR light source (AvaLight-HAL Tungsten Halogen) (>500 nm) and is equally split into two beams: one is directed to the slave channel of a PC driven double spectrophotometer (Ocean Optics USB SD2000) and the other is connected to a bifurcated optical fiber. The bifurcated optical fiber then guides the white light onto an appropriate reflective substrate spin coated with a thin polymer layer. At the same time the optical fiber collects the reflected beam, directing it to the master channel of the spectrophotometer. Each channel of the spectrophotometer is sensitive in the VIS-NIR spectrum with a resolution of 0.4 nm approximately.

The substrate should be totally reflective, at the spectrum used. Therefore standard silicon wafers constitute a reasonable choice. The accuracy of the method depends on the number of interference fringes in the recorded spectrum, as the existence of these extrema allows accurate fitting of the recorded spectrum and thus accurate calculation of the polymeric film thickness. In the case of thin polymeric films (e.g. 100 nm) on bare Si substrate no extrema appear on the reflectance spectrum. In order to obtain an adequate number of fringes within the reflectance spectrum, a thick transparent layer should be added in the film stack. With the Si processing it is easy either to grow a SiO_2 layer or deposit a Si_3N_4 film. In our study, the film stack includes thermally grown SiO_2 (wet oxidation at 1100 °C for 200 min, final SiO_2 thickness 1060 nm) on the Si substrate, prior to spin coating of the polymeric film.

By fitting the reflectance spectra to the interference equation, with known refractive indices of the layers employed, the film thickness can be calculated accurately. Under certain conditions this methodology could be also applied for the measurement of the refractive index [29]. However, the application of the WLRS methodology under the assumption of fixed refractive index (that of the polymeric matrix) constitutes an approximation, which under the conditions employed here is a satisfactory one. Indeed, the refractive index changes due to absorption/desorption of analytes at the concentration range studied here are very small (typically affecting values at the third decimal place). Such a small change in the refractive index does not affect the calculated film thickness and since we are interested in

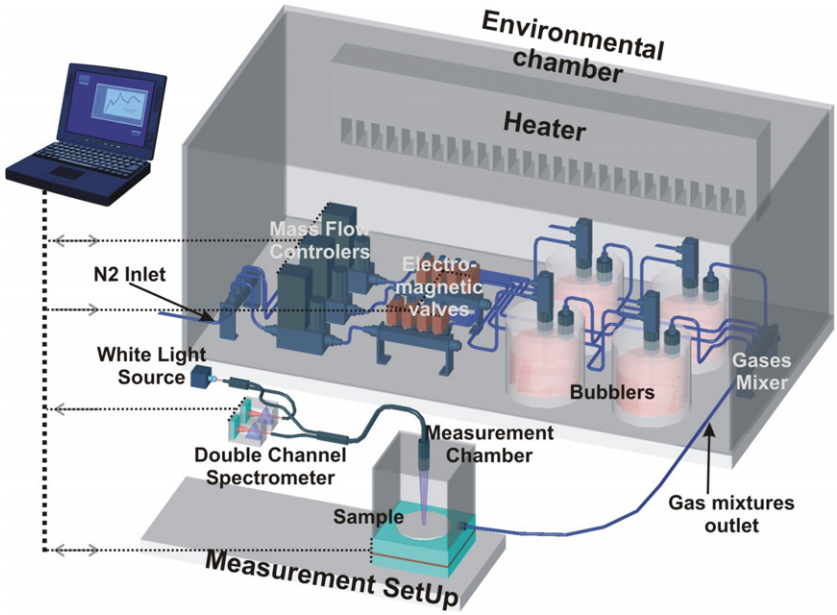

Fig. 2. Schematic representation of the measurement set-up.

real time monitoring of swelling/deswelling behavior, the refractive index of the polymeric film is considered constant throughout the measurement. The refractive index of the polymeric film for the spectrum of interest is calculated only once at the beginning of the experiment and the value obtained is used for all absorption/desorption steps with this polymer. Application of this method for every measured spectrum yields the temporal evolution of film thickness. At the same time, the spectrum of the light source recorded at the slave channel of the spectrophotometer, is used as a reference (multiplier in the interference equation) to adapt the theoretical approximation to the experimental data.

3. Results and discussion

3.1. Fabrication of the polymeric array

The polymers deposited with the proposed methodology should fulfil three criteria: (a) patterning capability, (b) complementary solubility parameters in order to form a polymer array covering a relatively wide solubility parameter range and (c) patterning compatibility i.e. the deposition of a polymeric area does not affect polymer areas already defined. As a result, a wide range of candidate polymers was considered experimentally and several of them, i.e. poly(hydroxyl ethyl methacrylate), hydroxyl terminated poly(dimethyl siloxane), AZ5214 positive conventional resist, poly(hydroxypropyl methacrylate), poly(butyl methacrylate) and poly(*n*-propyl methacrylate), were excluded from further study, because they did not fulfil the complete set of the aforementioned criteria.

The process for the deposition of the six films (Fig. 3) on the same substrate consists of the following sequence of steps:

(a) EPR spin coating on a silicon wafer, followed by a post apply bake step (PAB) for the evaporation of spin casting solvent, DUV exposure with the desired layout and post exposure bake (PEB) for cross-linking of the exposed areas. Removal of the unexposed regions with development follows; at the end of this step the EPR material has been lithographed in place.
(b) PDMS spin coating, post apply bake, exposure to DUV irradiation with the desired layout and new bake (PEB) for cross-linking of the exposed areas and removal of the unexposed regions.
(c) PMMA spin coating followed by DUV exposure and development.
(d) PHEMA negative, SAL-601 and UVIII are chemically amplified resists, so they are patterned in the same manner as EPR, PDMS.

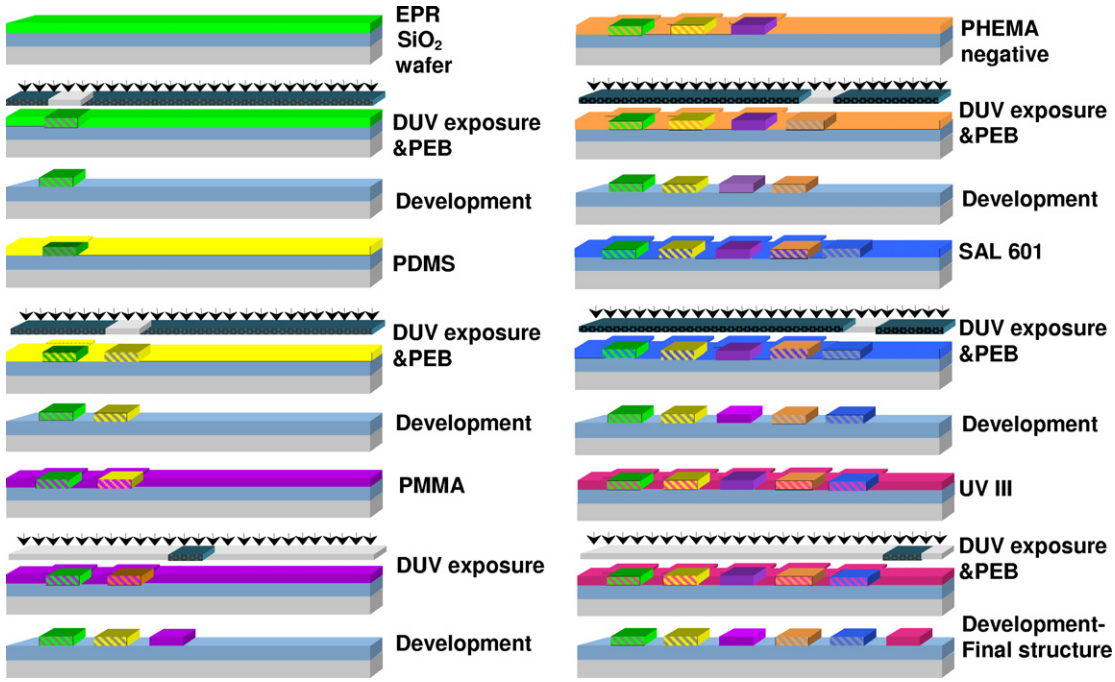

Fig. 3. Process flow for the fabrication of the polymeric array.

As regards to PHEMA, SAL-601 and UVIII the following should be noted: SAL-601 (a negative tone resist) and UVIII (a positive tone resist) are developed in aqueous base solutions, so we use a chemically amplified negative tone PHEMA instead of positive tone, pure PHEMA, as the first is more resistant during post-lithographic processing due to the formation of crosslinks. The lithographic steps of PHEMA negative, involve spin coating, baking, exposure, second baking and, finally, development in organic solvent contrary to pure PHEMA.

The details of the processing conditions applied for the fabrication of the array are listed in Table 1. At the end of the processing procedure, the structure obtained consists of six regions with six sensitive films on the same wafer. It must be noted that the material application sequence was engineered on the basis of the lithographic behavior of polymers employed and one cannot alter at will this sequence. The layout of each polymer area could be of any shape and resolution (at least in the range of several micrometers); however due to the size of the reflectance probe of the WLRS setup, in the present study each polymeric area is a rectangular area with larger dimensions $6 \times 10\ mm^2$.

3.2. Physical–chemical characterization of deposited polymers

The absorption/desorption for every polymeric film/analyte system is studied through film thickness changes during exposure of the polymeric film in the environment of the pre-selected analyte's concentra-

Table 1
Optimized lithographic conditions

Materials	Steps			
	PAB	Exposure time (s)	PEB	Development
EPR	100 °C, 5 min	7	3 min, 100 °C	PGMEA, 3 min
PDMS	120 °C, 5 min	450	120 °C, 4 min	MIBK, 9 min
PMMA	150 °C, 20 min	2500	–	MIBK-IPA 2:3, 5 min
PHEMA negative	120 °C, 15 min	500	120 °C, 5 min	MeOH, 1 min
SAL-601	105 °C, 10 min	70	105 °C, 2 min	TMAH, 8 min
UVIII	150 °C, 2 min	30	150 °C, 1 min	TMAH-H_2O 2:1, 1 min

tion (Fig. 4). In order to probe the sorption mechanism for each analyte/polymer pair, the measured equilibrium swelling $\delta L/L_0$ of polymeric films of the array exposed to five different activities of the four analytes was used to determine the sorption isotherm of each system (24 systems). L_0 is the initial polymer film thickness and δL is the increase in polymer film thickness after swelling due to the presence of analytes. Activities, a_s ($=p/p_{sat}$, where p_{sat} is the saturation pressure of the vapor at 30 °C), were determined from experimental data, as in Ref. [30]. The maximum activities probed for the analytes methanol, ethanol, water and toluene are 0.1852, 0.3873, 0.4777 and 0.4143 corresponding to concentrations of 40,000, 40,000, 20,000 and 20,000 ppm respectively. The estimation of polymer swelling at very low analyte activities or concentrations is possible through sorption isotherms. The resulting isotherms of the systems analytes-polymers are shown in Figs. 5a–d. We have recorded isotherms for all 24 polymer-analyte combinations, except for the system humidity-PDMS, as the swelling of the hydrophobic PDMS in the presence of humidity is negligible.

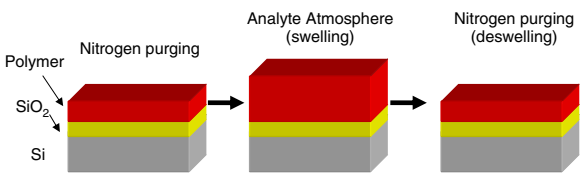

Fig. 4. Film thickness increase/decrease due to the absorption/desorption of analytes.

Among polymers deposited, PDMS is an elastomer while the remaining ones are glassy polymers. For PDMS and the methanol, ethanol and water analytes the level of sorption is low and a Henry law type of behavior is exhibited. For the highly absorbed toluene analyte and high activities (>0.2) there is a tendency for a Flory–Huggins type behavior (upward curvature). In the case of glassy polymers the additional feature exhibited is an early downwards curvature that might reflect absorption in pre-existing cavities that constitute the excess free volume of a glassy polymer matrix [31].

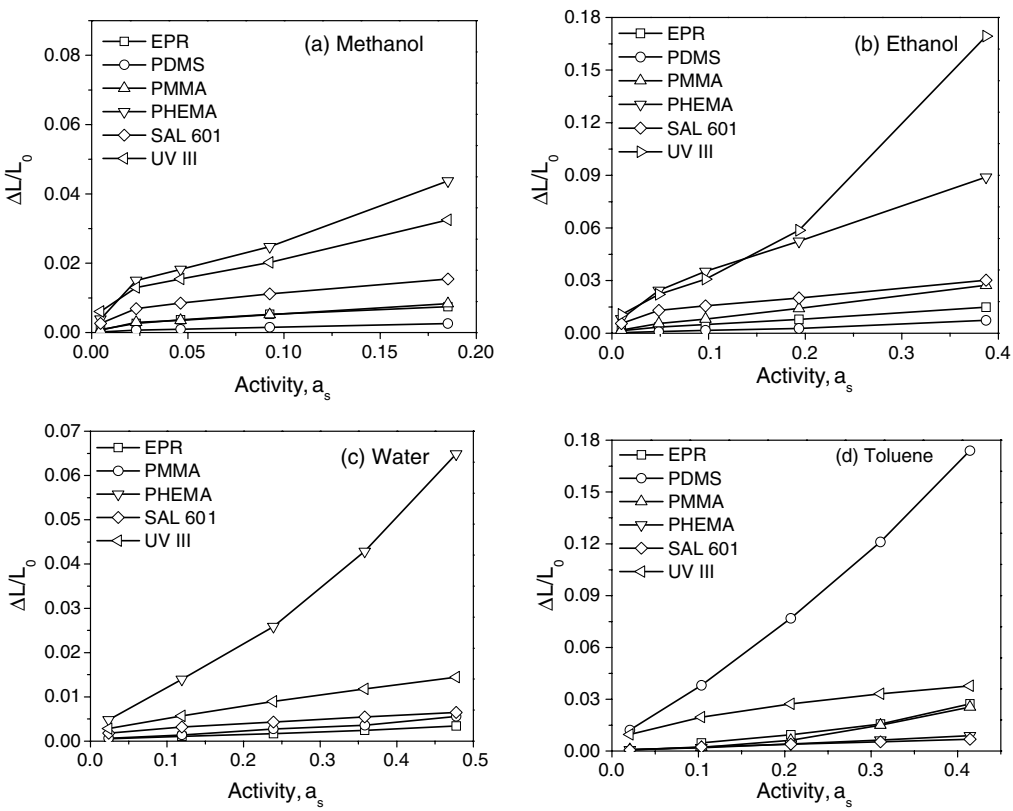

Fig. 5. Sorption isotherms of the four vapours in the polymers of the array.

The shape of the sorption isotherms of Fig. 5 is in line with those found in literature, by gravimetric methods, for free-standing bulk films [31–34]. On a quantitative basis, the analyte uptakes tend to be lower for the supported films case studied here, especially at higher activities and higher degrees of swelling, apparently because of partial suppression of volume swelling resulting from film attachment to the substrate.

Fabrication of chemical sensing arrays requires that a number of polymers with different solubility properties can be deposited on the substrate [35]. Such a choice aims at the enhancement of the selectivity and sensitivity of the array as the performance of each sensitive layer in the presence of analytes relates to the solubility parameters of the layer and respective compound [36]. In particular, a polymer is miscible with a low molecular weight solvent at room temperature, when, typically [37]:

$$\left|\delta_{\text{polymer}} - \delta_{\text{solvent}}\right| < 1.2\ (\text{cal/cm}^3)^{1/2} \quad (1)$$

where δ is the solubility parameter.

In order to cover a wide range of analytes, the polymers to be used should cover a substantial range of solubility parameter values; of course, the remaining two selection criteria mentioned in Section 3.1 (criteria (a) and (c)) should also be satisfied. The solubility parameters for the polymers employed in the sensor array have been estimated through the Hoy model [38], except for PDMS for which calculation is not possible (Hoy data for Si–O bond are not available), and its Hildebrand δ value ($= 7.5\ (\text{cal/cm}^3)^{1/2}$) is taken from general literature. The Hansen three-solubility parameters estimated by Hoy model and the experimental data from Hansen [37] are presented in Table 2. The solubility parameters of the analytes, from Hansen experimental data [37], appear in Table 3. The three solubility parameters are related to Hildebrand total parameter by the equation;

$$\delta^2 = \delta_{\text{D}}^2 + \delta_{\text{P}}^2 + \delta_{\text{H}}^2 \quad (2)$$

where δ_{D}, δ_{P}, δ_{H} are contributions from the non-polar interaction, polar interaction and hydrogen bonding respectively. Therefore, the polymer array used covers the $[7.5–11.8\ (\text{cal/cm}^3)^{1/2}]$ solubility range. This range combined with Eq. (1) suggests a capacity for detectable swelling for analytes in the $[6.3–13.0\ (\text{cal/cm}^3)^{1/2}]$ solubility range; actually the range on the high δ side is wider (see below). In Fig. 6, an axis of the solubility parameters of the polymer materials and analytes used during measurements is depicted.

Table 2
Solubility parameter (Hoy model) values of polymeric materials in $(\text{cal/cm}^3)^{1/2}$ units

Polymeric materials	δ_{H}	δ_{P}	δ_{D}	δ_{total}
PMMA	5.1	4.5	6.6	9,5
UVIII	3.6	5.0	7.5	9.7
SAL-601	2.4	5.8	8.5	10.6
EPR	5.4	4.5	8.9	11.4
PHEMA	7.2	6.4	6.9	11.8

Table 3
Solubility parameter values of analytes in $(\text{cal/cm}^3)^{1/2}$ units

Analytes	δ_{H}	δ_{P}	δ_{D}	δ_{total}
Toluene	1	0.7	8.8	8.9
Methanol	10.9	6.0	7.4	14.5
Ethanol	9.5	4.3	7.7	13.0
Water	20.7	7.8	7.6	23.4

Fig. 7 shows the response of the full polymer array to all analytes at 5000 ppm; the equilibrium time is small (typically, ca. 2 min), as a result of the low polymer film thickness. Putting aside the case of water (for which δ based approaches are known to fail for polymers), we find that our 1D δ-value approach (Fig. 6) is qualitatively compatible for a satisfactory portion of our absorption data. Yet, substantial deviations are observed for some of the analytes and the EPR, PMMA, SAL-601 and UVIII polymers. Major deviation cases are the following:

(a) PMMA shows limited response to toluene, a known solvent of the polymer ($|\delta_{\text{PMMA}} - \delta_{\text{toluene}}| = 0.6\ (\text{cal/cm}^3)^{1/2}$).

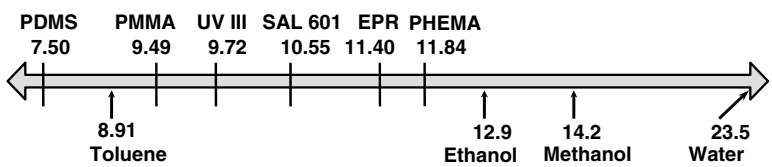

Fig. 6. Solubility parameters of polymeric materials and analytes.

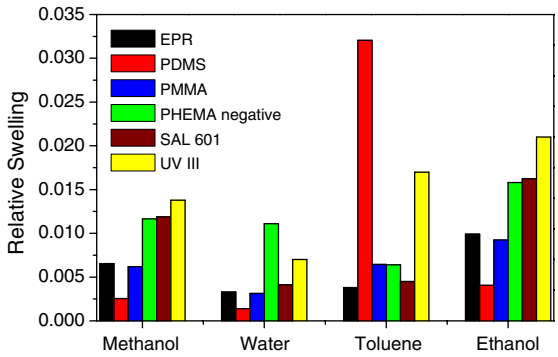

Fig. 7. Swelling response at equilibrium of the six-polymer array to methanol, ethanol, toluene vapors and humidity at 5000 ppm.

(b) SAL-601 absorbs similarly to PHEMA, except for water, in spite of their different δ-values.
(c) UVIII responds more strongly to ethanol than to toluene though $(|\delta_{\mathrm{UVIII}} - \delta_{\mathrm{toluene}}| = 0.8\ (\mathrm{cal/cm^3})^{1/2}$, while $(|\delta_{\mathrm{UVIII}} - \delta_{\mathrm{ethanol}}| = 3.3\ (\mathrm{cal/cm^3})^{1/2}$.
(d) The swelling capacity of EPR is limited compared to that of PHEMA despite the similar δ-values of the two polymers; yet this might be partly due to the different levels of crosslinking.

Deviations are hardly surprising as, for example, some of the polymers employed bear polar or capable of hydrogen bonding groups while others do not. In order to probe the nature of deviations we now use the 3D δ-value approach, which takes into account separate groups contributions (Eq. (2)). A typical solubility criterion is the following [37];

$$(R_a)^2 = 4(\delta_{D1} - \delta_{D2})^2 + (\delta_{P2} - \delta_{P1})^2 + (\delta_{H2} - \delta_{H1})^2 \leq 3.4\ (\mathrm{cal/cm^3})^{1/2} \quad (3)$$

where R_a is a modified difference between the Hansen solubility parameter for a solvent (1) and polymer (2). Yet, even this is not a fully satisfaction criterion, as Hansen admits [37]. Upon application of Eq. (3) we find that:

(a) Some of the deviations experienced with the 1D approach cease to occur; examples of problems resolved are reflected in the following $(R_a)^2$ values:

$(R_a)^2_{\mathrm{EPR-methanol}} = 6.4\ (\mathrm{cal/cm^3})^{1/2}$,
$(R_a)^2_{\mathrm{EPR-ethanol}} = 4.8\ (\mathrm{cal/cm^3})^{1/2}$ and
$(R_a)^2_{\mathrm{PMMA-toluene}} = 7.1\ (\mathrm{cal/cm^3})^{1/2}$.

(b) Other deviations remain present; major examples of remaining problems are reflected in the following $(R_a)^2$ values:

$(R_a)^2_{\mathrm{SAL-601-methanol}} = 8.8\ (\mathrm{cal/cm^3})^{1/2}$ vs.
$(R_a)^2_{\mathrm{SAL-601-ethanol}} = 7.4\ (\mathrm{cal/cm^3})^{1/2})$ and
$(R_a)^2_{\mathrm{UVIII-methanol}} = 7.4\ (\mathrm{cal/cm^3})^{1/2})$ vs.
$(R_a)^2_{\mathrm{UVIII-ethanol}} = 6.0\ (\mathrm{cal/cm^3})^{1/2})$.

Situations falling into case (b) may either reflect problems intrinsic to the δ-approach or can be due to a kinetic contribution. Yet, it might not be without significance that major case (b) examples correspond to commercial products for which formulation is only approximately described by the structures presented in Fig. 1.

3.3. Processing effect on the swelling properties of the patterned areas

During the fabrication of the polymeric array each polymeric film undergoes the processing steps of the following layers. The areas covered with negative tone chemically amplified resists SAL-601, PHEMA negative, PDMS and EPR are subjected to DUV exposure and PEB and then dipped in the developer solution, while areas covered with the positive tone UVIII and PMMA need not be exposed, but do undergo development. These processing steps could in principle affect the swelling properties of the polymeric films. Fig. 8 shows the relative swelling (at 5000 ppm of methanol, ethanol, toluene and water) of two polymeric materials (PHEMA, SAL-601) of the array, after each of the following processing steps: (1) spin coating, (2) exposure and PEB, (3) development. In most cases an increase in the swelling response after the development step is observed. This increase in the swelling response is not unexpected and could be attributed to the penetration of the developer molecules during the development step. The above hypothesis is supported by the PEB results which suggest that the monitored swelling response is the same as for unprocessed samples.

As it was described in Section 2.2, the polymeric array is fabricated in the same substrate using lithographic processes. Consequently, all polymers except for the last (UVIII) are also subjected to the processing steps necessary for the deposition of the remaining materials of the array. The effect of multiple lithographic processes is studied by sorption measurements of the polymers deposited

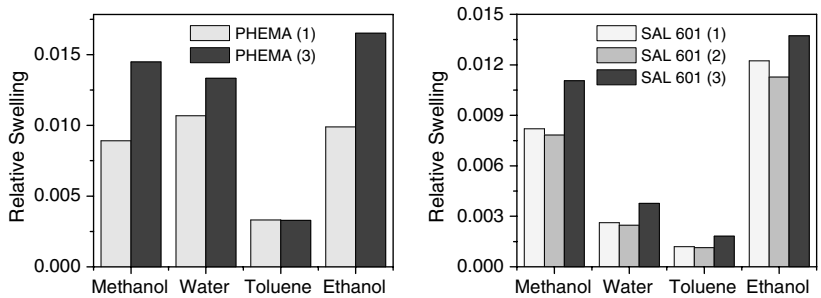

Fig. 8. Effect of lithographic steps on SAL-601 and PHEMA swelling.

in separate substrates. The resulting relative swelling values compared to those of the array for three materials (PDMS, PHEMA, UVIII) are depicted in Fig. 9. PDMS swelling ability (Fig. 9a) does not change although it undergoes four additional depositions. In PHEMA case (Fig. 9b), a decrease in vapors sorption is observed in all cases except for toluene. UVIII response is presented in Fig. 9c for comparison. In general, polymers sorption exhibits some limited variation, while the relative analyte selectivity is not affected.

3.4. Repeatability study and effect of analytes sequence

A crucial parameter for a sensor is its ability to provide the same results at the measurement of the same quantity over long time. For that purpose, the response of the EPR polymeric material was studied over a three-month period. The results are depicted in Fig. 10 and show that the swelling ability of the same film of EPR changes negligibly and its response to all vapors studied remains constant. It should be noted that the sample was kept in humidity-free environment during this period of time. Consequently, the physicochemical properties of the deposited polymer are rather stable over time.

During the sorption measurements of the array, the four analytes are introduced to the measurement chamber in specific sequences. In order to study the effect of analyte sequence on polymer response, swelling measurements were performed using the same polymeric film (PHEMA) and five sufficiently different analyte sequences (Table 4). The sample was exposed to each analyte for 40 min and then was purged with dry nitrogen for another 40 min

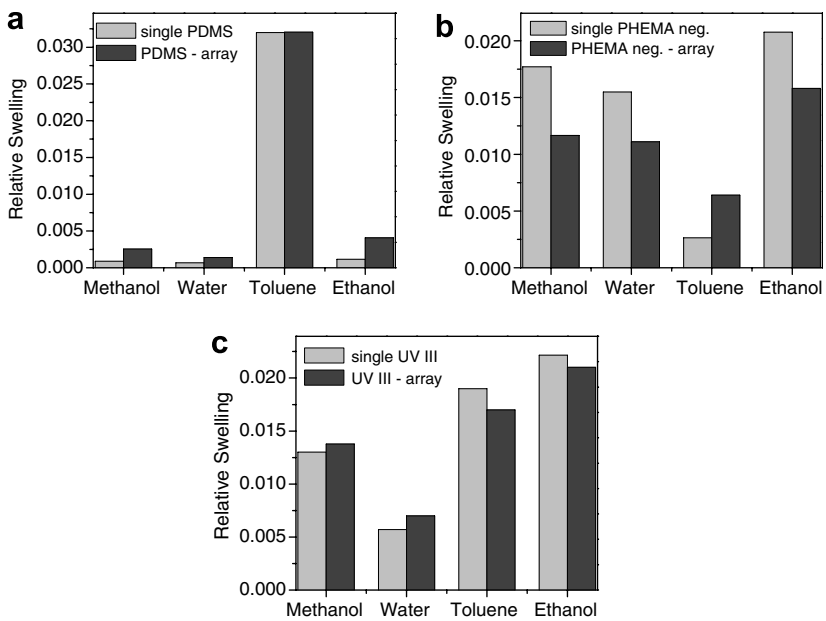

Fig. 9. Effect of multiple lithographic depositions in swelling properties of PDMS and PHEMA negative.

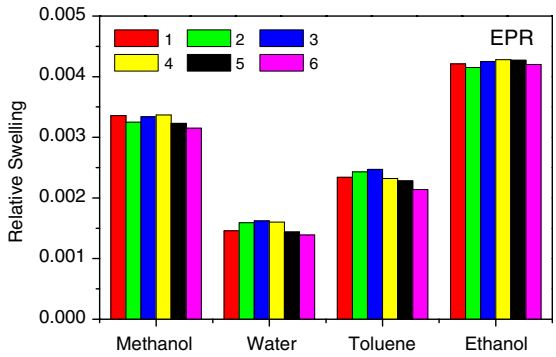

Fig. 10. Relative swelling results of the same EPR film in a period from the first measurement (weeks); (1) 0, (2) 1, (3) 4, (4) 9, (5) 11, and (6) 13.

before the insertion of the next analyte. Between the different sequences, the film was purged with dry nitrogen for 2 h.

For different sequences and a given analyte the relative swelling values show a variation of ca. $\pm$ 10 % around the average. On the other hand, the reproducibility of each value (for a given sequence and analyte) is ca. $\pm$ 2 %. As $2\% \ll 10\%$, we conclude that the variation seen in Fig. 11 for a given analyte as a function of the analyte sequence reflects true trends and not random variations. As a general explanation, we suggest that despite the application of full desorption steps between the introduction of the successive analytes of a given sequence, the matrix exhibits a short-term memory of the chain rearrangements resulting from the sorption and desorption processes. We will now consider the observed trends in terms of simple parameters.

Table 4
Combinations in the analytes sequences

Series	Analytes			
1st	Methanol	Water	Toluene	Ethanol
2nd	Water	Ethanol	Methanol	Toluene
3rd	Water	Methanol	Ethanol	Toluene
4th	Toluene	Ethanol	Methanol	Water
5th	Toluene	Water	Methanol	Ethanol

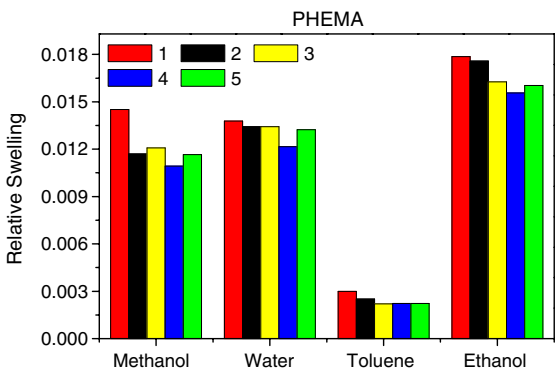

Fig. 11. Swelling response of PHEMA at the presence of five analytes sequences.

The maxima and minima of relative swelling levels for each analyte are as follows:

(a) Maxima for all analytes correspond to the 1st sequence.
(b) Minima for methanol, water, and ethanol correspond to the 4th sequence. In the case of toluene the same, within experimental error, minimum value is observed for the 3rd, 4th and 5th sequences.

We see that all maxima correspond to a single sequence (1st sequence) while there is a strong correlation between minimum values and another sequence (4th sequence). This clustering of extreme values strengthens our conclusion that the variation of relative swelling value observed for each analyte is not a random one. The 4th sequence corresponds to increasing delta values; yet an improved insight results upon noting that toluene is the analyte with the least swelling capacity for the polymer tested (PHEMA). Consequently, toluene facilitates the least, through chain rearrangement, the hosting of the remaining analytes by the matrix. Nevertheless, it is to be expected that the exact sequence of the remaining analytes plays some role as well; we note that the 5th sequence compared to 4th sequence (both having toluene as the 1st analyte) leads to enhanced swelling levels. Yet, none of the values found for the 5th sequence exceeds those found for the remaining sequences (1st, 2nd and 3rd). Observations of that type can be generalized in the form of a qualitative guideline: each full sequence of analytes corresponds to a small but persistent deviation from average response; the effect of the first analyte is stronger than that of the remaining analytes.

The above suggest that the trends of the data presented in Fig. 11 can be understood satisfactorily in terms of simple parameters; yet, simple parameters need not be able to fully capture the fine details of response patterns.

4. Conclusions

This work demonstrates a novel process which takes advantage of photolithographic techniques

and allows for the deposition of chemical sensor array of six polymers with distinct sensing properties. Most analytes in the [6.3–13.0 $(cal/cm^3)^{1/2}$] solubility range and beyond (high δ side) can be detected. The response of each polymer of the array is in reasonable accordance with expectations based on solubility parameters, while processing introduces only a limited change to the sensing properties of the deposited polymers. Persistent long term performance is demonstrated. Finally, the sequence of analytes was found to have a limited only and non-random effect on the levels of sorption; main pertinent trends can be understood on the basis of simple physical chemical considerations.

Acknowledgements

Authors would like to thank Dr. P. Argitis (NCSR 'Demokritos') and Dr. M. Sanopoulou (NCSR 'Demokritos') for helpful discussions.

References

[1] Muñoz-Aguirre S, Nakamoto T, Moriizumi T. Sensor Actuat B 2005;105:144–9.
[2] Nagle HT, Gutierrez-Osuna R, Schiffman SS. IEEE Spect 1998;35:22–31.
[3] Mabrook MF, Pearson C, Petty MC. Sensor Actuat B 2006;115:547–51.
[4] Albert KJ, Lewis NS, Schauer CL, Sotzing GA, Stitzel SE, Vaid TP, et al. Chem Rev 2000;100:2595–626.
[5] Quercia L, Loffredo F, Alfano B, La Ferrara V, Di Francia G. Sensor Actuat B 2004;100:22–8.
[6] Patel SV, Mlsna TE, Fruhberger B, Klaassen E, Cemalovic S, Baselt DR. Sensor Actuat B 2003;96:541–53.
[7] Sepaniak M, Datskos P, Lavrik N, Tipple C. Anal Chem 2002;74:568–75.
[8] Maute M, Raible S, Prins FE, Kern DP, Ulmer H, Weimar U, et al. Sensor Actuat B 1999;58:505–11.
[9] Kim BH, Prins FE, Kem DP, Raible S, Weimar U. Sensor Actuat 2001;78:12–8.
[10] Baller K, Lang HP, Fritz J, Gerber Ch, Gimzewski JK, Drechsler U, et al. Ultramicroscopy 2000;82:1–9.
[11] Chatzandroulis S, Tegou E, Goustouridis D, Polymenakos S, Tsoukalas D. Sensor Actuat B 2004;103:392–6.
[12] Hierlemann A, Brand O, Hagleitner C, Baltes H. Proc IEEE 2003;91:839–63.
[13] Tekin E, de Gans BJ, Schubert US. Mater J Chem 2004;14:2627–32.
[14] Deng Z, Stone DC, Thompson M. Analyst 1996;121:671–9.
[15] Chang SM, Iwasaki Y, Suzuki M, Tamiya E, Karube I, Muramatsu H. Anal Chim Acta 1991;249:323–9.
[16] Ricco AJ, Crooks RM, Osbourn GC. Acc Chem Res 1998;31:289–96.
[17] Sugimoto I, Nakamura M, Kuwano H. Sensor Actuat B 1996;37:163.
[18] Sugimoto I, Nakamura M, Kuwano H. Sensor Actuat B 1993;10:117–22.
[19] Dutta P, Senesac LR, Lavrik NV, Datskos PG, Sepaniak MJ. Sensor Lett 2004;2:238–45.
[20] McGill RA, Chung R, Chrisey DB, Dorsey PC, Matthews P, Pique A, et al. IEEE Trans Ultrason, Ferroelec, Freq Contr 1998;45:1370–80.
[21] Grate JW, Nelson DA. Proc IEEE 2003;91:881–9.
[22] Goustouridis D, Manoli K, Chatzandroulis S, Sanopoulou M, Raptis I. Sensor Actuat B 2005;111–112:549–54.
[23] Argitis P, Raptis I, Aidinis CJ, Glezos N, Baciocchi M, Everett J, et al. Vac Sci Technol B 1995;13:3030–4.
[24] Tserepi A, Cordoyiannis G, Patsis GP, Constantoudis V, Gogolides E, Valamontes ES, et al. Vac Sci Technol B 2003;21:174–82.
[25] Olzierski A, Raptis I. Microelectron Eng 2004;73–74:244–51.
[26] Vasilopoulou M, Boyatzis S, Raptis I, Dimotikalli D, Argitis P. J Mater Chem 2004;14:3312–20.
[27] Gentili M, Gerardino A, Fabrizio ED. J Appl Phys 1998;37:4632–5.
[28] Ito H, Breyta G, Hofer D, Sooriyakumaran R. American Chemical Society PMSE 1995;72:144.
[29] Spuller MT, Perchuk RS, Hess DW. J Electrochem Soc 2005;152:G40.
[30] Manoli K, Goustouridis D, Chatzandroulis S, Raptis I, Valamontes ES, Sanopoulou M. Polymer 2006;47:6117–22.
[31] Dimos V, Sanopoulou M. J Appl Polym Sci 2005;97:1184–95.
[32] Connelly RW, McCoy NR, Koros WJ, Hopfenberg HB, Steward ME. J Appl Polym Sci 1987;34:703–19.
[33] Rodriguez O, Fornasiero F, Arce A, Radke CJ, Prausnitz JM. Polymer 2003;44:6323–33.
[34] Sun Y-M, Lee H-L. Polymer 1996;37:3915–9.
[35] James D, Scott SM, Ali Z, O'Hare WT. Microchim Acta 2005;149:1–17.
[36] Grate JW, Abraham MH. Sensor Actuat B 1991;3:85–111.
[37] Hansen CM. Hansen solubility parameters, a user's handbook. Florida: CRC Press; 2000.
[38] Hoy KL. J Paint Technol 1970;42:76.